Journal of Korea Multimedia Society Vol. 17, No. 12, December 2014(pp. 1412-1417)
http://dx.doi.org/10.9717/kmms.2014.17.12.1412

Implementation of 2D Snake Model-based Segmentation on Corpus Callosum

Ala'a ddin Al Shidaifat[†], Heung-Kook Choi[††]

ABSTRACT

The corpus callosum is the largest part of the brain, which is related to many neurological diseases. Snake model or active contour model is widely used in medical image processing field, especially image segmentation they look into the nearby edge, localizing them accurately. In this paper, corpus callosum segmentation using the snake model, is proposed. We tested a snake model on brain MRI. Then we compared the result with an active shape approach and found that snake model had better segmentation accuracy also faster than active shape approach.

Key words: Corpus Callosum; Snake; Active Shape Approach; Segmentation.

1. INTRODUCTION

The corpus callosum has been known as one of the largest white matter structures in the human brain. It is also known as the colossal commissure, which plays an essential role in relaying sensory, motor and cognitive information from homologous regions in the two hemispheres. Various medical researchers have shown that the size and shape of the corpus callosum are correlated to sex, age, brain growth and degeneration, handedness, and musical ability. In particular, abnormalities in the volume and architecture of the corpus callosum are related to many neurological disorders, such as bipolar and unipolar disorders, attention deficit hyperactivity disorder, autism, mental retardation, schizophrenia [1], developmental language disorders, and Alzheimer disease.

Actually the intensity of corpus callosum in magnetic resonance (MR) images is very different from its surroundings. On the other hand, it's similar brightness with another part of the brain located in the sagittal region called the fornix, so it's hard to recognize its local shape.

The development of medical imaging technologies in last three decades has grown and enormously increased its important in the diagnosis of diseases [2]. Segmentation of brain structures is a critical task in medical image analysis various methods in previous researches have been applied to the segment corpus callosum from the brain MR image. Schonmeyer et. al. present an algorithm based on the so-called Definiens Cognition Network Technology from Definiens and extends [3]. Freits et. al. used watershed transform [4], which is performed on the fractional anisotropy (FA) map weighted by the projection of the principal eigenvector in the left-right direction. Zadeh et. al. proposed methods for segmentation of corpus callosum using diffusion tensor imaging [5], and

※ Corresponding Author : Heung-Kook Choi, Address: (621-749) 197 Injero, Gim-Hae, Gyeong-Nam, Korea, TEL : +82-55 320-3437, FAX : +82-55 322-3107, E-mail : cschk@inje.ac.kr
Receipt date : July 14, 2014, Revision date : Oct. 6, 2014
Approval date : Oct. 27, 2014
[†] Department of Computer Engineering, UHRC, Inje University, Korea (E-mail : alaaddinsh@hotmail.com)
[††] Department of Computer Engineering, UHRC, Inje University, Korea
※ This research was supported by Basic Science Research Program through the National Research Foundation of Korea (NRF) funded by the Ministry of Education, Science and Technology (2012-0002646).

Seixas et. al. used previous knowledge on statistical models to the segment corpus callosum automatically [6].

Active shape models (ASMs) are statistical models of the shape of objects which iteratively deform to fit to an example of the object in a new image, developed by Tim Cootes and Chris Taylor [7]. The model has similarities with the active contour models or snakes, but differs in that global shape constraint are applied.

In this work, another approach of corpus callosum segmentation called snake model is performed. Kass et. al. was introduced the original snake model by [8], which defines a curve within an image evolving through an internal force from the inside of the curve and external force computed from the image data, to segment the targeted object.

The rest of this paper is organized in three more sections. Section 2 explains the snake model. Section 3 describes our practical experiments and presents the implementation details, evaluates our results by comparing it to related work results. Final considerations and future works are presented in Section 4.

2. SNAKE MODEL

The snake is an energy minimizing parametric contour deforms over a series of time steps or iteration. Consequently each element x along the contour depends on two parameters as in (1), which is c curve (space) parameter and commonly varies between 0 and 1, is t iteration (time) parameter.

$$x = x(c,t) \tag{1}$$

The total energy of the model is defined as sum of the energy for the individual snake elements:

$$E_{snake} = \int_0^1 E_{element}(x(c))dc \tag{2}$$

The integral notation used in (2) implies an open-ended snake; but joining the first and last elements makes the snake into a closed loop as shown in Fig. 1.

Over a series of time steps the snake moves into alignment with the nearest edge. The contour is determined by three forces or constrains; internal, external, and image. Internal constrains give the model elasticity and rigidity, external constraints come from initialization procedures. Image energy is pushing the model towards the edges. We can rewrite the (2) in terms of three basic energy functions:

$$E_{snake} = \int_0^1 E_{\text{int}ernal}(x)dc + \int_0^1 E_{external}(x)dc + \int_0^1 E_{image}(x)dc \tag{3}$$

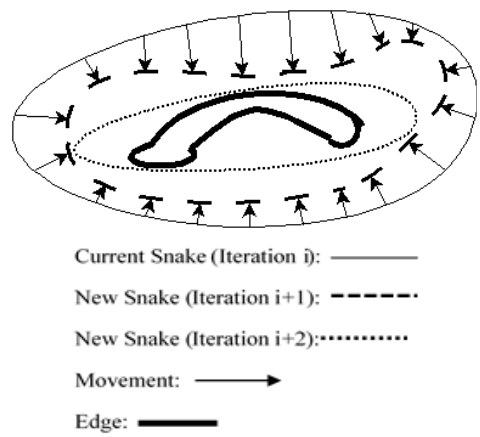

Fig. 1. A closed active contour model.

2.1 Internal energy

The below equations defined the internal energy of a snake model. This energy contains two order terms; first-order term and second-order terms controlled by $\alpha(c)$ and $\beta(c)$ respectively.

$$E_{\text{int}ernal} = E_{Elasticity} + E_{Rigidity} \tag{4}$$

$$E_{Elasticity} = \alpha(c)|x_c(c)|^2 \tag{5}$$

$$E_{Rigidity} = \beta(s)|x_c(c)|^2 \tag{6}$$

The first-order term makes the snake act like a rubber band representing elasticity; the second-order term makes it resist bending by producing rigidity in [9] and [10].

If the other terms were not given the contour it will keep shrinking to a single spot. Changing

the weights $\alpha(c)$ and $\beta(c)$ controls the relative importance of the elasticity and rigidity terms. If we set $\beta(s)$ to zero meaning that the second order is continuous will the model to have a corner.

2.2 External energy

The external energy of a snake model discussed by Xu and Prince in [11], it is responsible for putting the snake near the desired local minimum [8], the initialization procedures are applied to control both of attraction and repulsion forces which hold the active contour models to or from the desired features. The external energy term representing the attraction and repulsion in the next equation respectively:

$$E_{external}(x) = k|i-x|^2 \tag{7}$$

$$E_{external}(x) = \frac{k}{|i-x|^2} \tag{8}$$

The attraction force we can say it is like spring force and the repulsion energy like a volcano pushing out. They are generated between a snake element and a point i in an image. In the attraction force case the energy is minimal when $x=i$, and it takes the value of k when $i-x=\pm 1$, but in the repulsion energy case the energy is maximum when $x=i$. The repulsion term must be stopped as $i-x\rightarrow 0$.

2.3 Image (Potential) energy

There are three image energies E_{image}; lines, edges and terminations. It is produced by the processing of the image $I(x,y)$ results a force that is used to control snakes towards the features of interest. The total image energy can be expressed as a weighted combination of lines, edges and termination functions:

$$P = E_{image} = w_{line}E_{line} + w_{edge}E_{edge} + w_{term}E_{term} \tag{9}$$

The lines, edges and terminations energy shown in the next equation respectively:

$$E_{line} = \int_0^1 I(x(c))dc \tag{10}$$

$$E_{edge} = -\left|\nabla I(x(c))\right|^2 \tag{11}$$

$$E_{term} \equiv \int_0^1 \frac{\partial\theta}{\partial n_\perp}dc = \int_0^1 \frac{\partial^2 C/\partial n^2{}_\perp}{\partial C/\partial n}dc \tag{12}$$

$$E_{term} = \int_0^1 \frac{C_{yy}C_x^2 + C_{xx}C_y^2 - 2C_{xy}C_xC_y}{\left(C_x^2+C_y^2\right)^{3/2}}dc \tag{13}$$

3. EXPERIMENTAL RESULTS

The brain images were acquired using a Siemens 3T MR imaging scanner from Pusan National University Hospital, Pusan South Korea. The subjects were 24-27 years old normal male. Fig. 2, first column shows the test images, which are a T1-weighted grayscale DICOM image with a 256×256 resolution. Fig. 2, the second column shows the results of corpus callosum segmentation using the snake model.

The initial points are placed around the corpus callosum boundary manually by the user, the corpus callosum can be segmented accurately. The initialization can be placed far from the corpus callosum, if there are no fake edges interrupt between initialization and corpus callosum boundary. The segmentation result of snake model depends on several weight energy parameters. In our experiment we set them as follows:

- The elasticity controls the first derivative term of contour, $\alpha(s)=10^{-3}$
- The rigidity controls the second derivative term of contour, $\beta(s)=0.34$
- The weighting factor for intensity, edge and terminate based on potential terms, $w_{line}=0$, $w_{edge}=3$, $w_{term}=0$.

The number of iterations were controlling the segmentation accuracy.

To evaluate the corpus callosum segmentation of snake model, we used Jaccard coefficient measurement in [12]. Jaccard coefficient can be computed based on the number of elements in the intersection set divided by the number of elements in the union set. The ground truth for validation

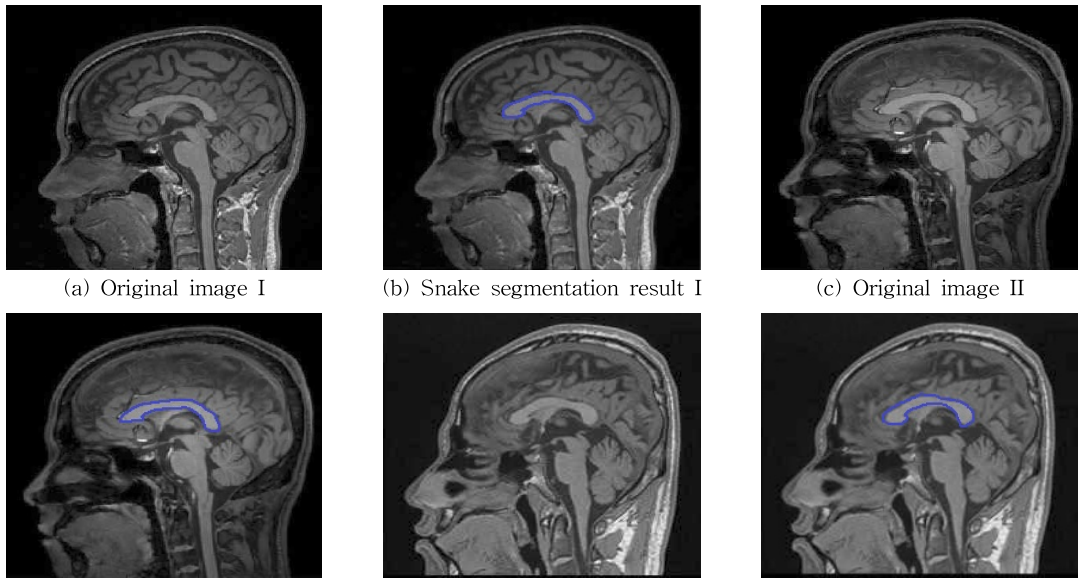

(a) Original image I (b) Snake segmentation result I (c) Original image II

(d) Snake segmentation result II (e) Original image III (f) Snake segmentation result III

Fig. 2. The first column: Original images; Second column: The segmentation results of Snake.

of segmentation results were manually drawn by ITKSNAP 1.6 [13]. The segmentation is matched to the manuals provided ground truth according to the next equation.

$$P(A,B)=\frac{|A\cap B|}{|A\cup B|}\times 100\% \tag{14}$$

where $P(A, B)$ represents the segmentation accuracy in percentage, A and B represent the binary images of ground truth and segmentation result of target corpus callosum respectively.

In the Fig. 3, the first column shows the ground truth for validation of segmentation results. The

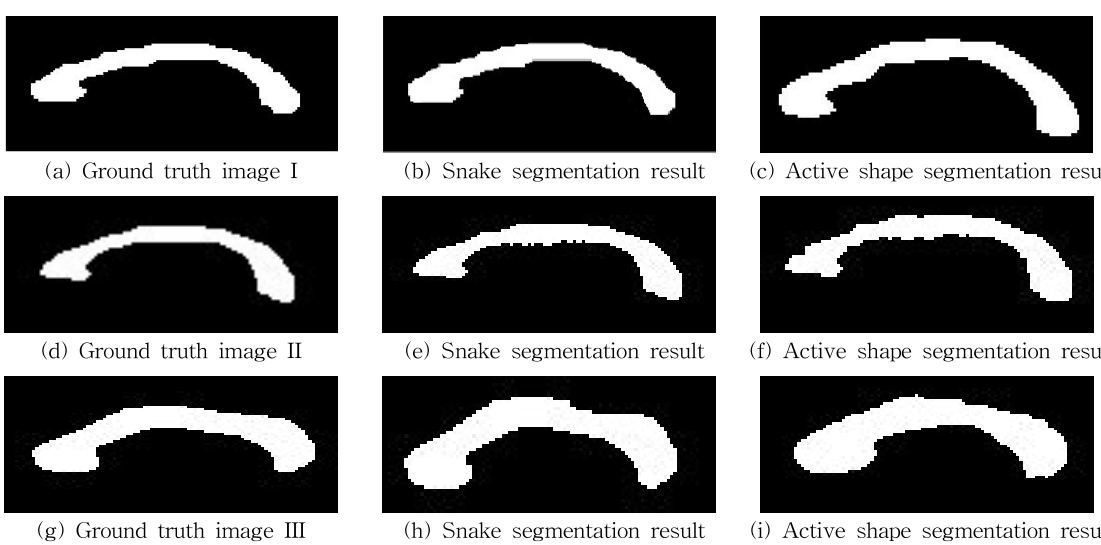

(a) Ground truth image I (b) Snake segmentation result (c) Active shape segmentation result

(d) Ground truth image II (e) Snake segmentation result (f) Active shape segmentation result

(g) Ground truth image III (h) Snake segmentation result (i) Active shape segmentation result

Fig. 3. The first column: the ground truth of the corpus callosum, Second column: result of snake model, third column: the result of active shape approach.

Table 1. Comparison of snake model and active shape model

	Accuracy of segmentation (%)		Elapsed time (Sec)	
	Snake	*ASM*	*Snake*	*ASM*
Original image Ⅰ	91.51	80.53	12.32	14.59
Original image Ⅱ	92.83	73.01	14.14	16.21
Original image Ⅲ	91.05	80.93	13.22	10.47
Original image Ⅳ	91.47	79.52	13.33	15.07
Original image Ⅴ	91.38	87.60	13.52	15.23

second column shows the binary images of snake model results and the third column shows the binary images results of the active shape approach segmentation [14].

Comparison of segmentation accuracy and elapsed time of snake model and ASM (Active shape model) is shown in Table 1.

4. CONCLUSION

In this paper, we applied the snake model to the segment corpus callosum from brain MR images, which were provided from Pusan National University hospital, Pusan South Korea. We compared our segmentation results with the results of the active shape approach by referring to the ground truth of the corpus callosum. It was clearly shown that the snake model is faster than ASM except in the third image in the Fig. 2(e). The intensity of corpus callosum in the third image is quite different from its surroundings. So it was easier to determine its local shape. On the other hand, the segmentation accuracy of snake model was much better than that of ASM. The snake segmentation accuracy was 91 ~93%, while ASM accuracy 73~80%. Nevertheless, a snake model still needs to be optimized and also the ground truth of the corpus callosum should be segmented by the expert.

REFERENCES

[1] M.S. Keshavan, V.A. Diwadkar, K. Harenski, D.R. Rosenberg, J.A. Sweeney, and J.W. Pettegrew, "Abnormalities of the Corpus Callosum in First Episode, Treatment Naive Schizophrenia," *Journal of Neurology, Neurosurgery and Psychiatry,* Vol. 72, No. 6, pp. 757-760, 2002.

[2] N. Sengee, A. Sengee, A. Enkhbolor, and H.K. Choi, "Contrast Enhancement for Segmentation of Hippocampus on Brain MR Images," *Journal of Korea Multimedia Society,* Vol. 15, No. 12, pp. 1409-1416, 2012.

[3] R. Schönmeyer, M. Athelogou, A.R. Jagiela, C. Haenschel, and D.E.J. Linden, *Fully Automated Segmentation of Corpus Callosum from Sagittal MRT Images,* Definiens the Tissue Phenomics Company, Munich, Germany, SPL-0006-01-260208.

[4] P. Freitas, L. Appenzeller, and R. Lotufo, "Watershed-Based Segmentation of the Midsagittal Section of the Corpus Callosum in Diffusion MRI," *IEEE Conference on Graphics, Patterns and Images,* pp. 274-280, 2011.

[5] M.R.N. Zadeh, S. Saksena, A.B. Fermi, Q. Jiang, H.S. Zadeh, M. Rosenblum, et al., "Segmentation of Corpus Callosum using Diffusion Tensor Imaging: Validation in Patients with Glioblastoma," *BMC Medical Imaging,* Vol. 12, No. 10, pp. 1471-2342, 2012.

[6] F.L. Seixas, A.S.D. Souza, A.A.S. Santos, and D.C.M. Saade, "Automated Segmentation of the Corpus Callosum Midsagittal Surface Area," *IEEE Conference on Computer Graphics and Image Processing,* pp. 287-293, 2007.

[7] T.F. Cootes, C.J. Taylor, D.H. Cooper, and J. Graham, "Active Shape Models-Their Training And Application," *Computer Vision and Image Understanding*, Vol. 61, No. 1, pp. 38-59, 1995.

[8] M. Kass, A. Witkin, and D. Terzpoulos, "Snakes: Active Contour Models," *International Journal of Computer Vision,* Vol. 1, No. 4, pp. 321-331, 1988.

[9] B. Ostlad and A. Tonp, "Encoding of a Priori Information in Active Contour Models," *IEEE Transactions on Pattern Analysis and Machine Intelligence*, Vol. 18, No. 9, pp. 863-872, 1996.

[10] S.C. Zhu and A. Yuille, "Region Competition: Unifying Snakes, Region Growing, and Bayes/MDL for Multiband Image Segmentation," *IEEE Transations on Pattern Analysis and Machine Intelligence*, Vol. 18, No. 9, pp. 884-900, 1996.

[11] C. Xu and J. Prince, "Snakes, Shapes, and Gradient Vector Flow," *IEEE Transactions on Image Processing*, Vol. 7, No. 3, pp. 359-369, 1998.

[12] C. Held, R. Palmisano, L. Haberle, and T. Wittenberg, "Comparison of Parameter-adapted Segmentation Methods for Fluorescence Micrographs," *Cytometry Part A.,* Vol. 79, No. 11, pp. 933-945, 2011.

[13] ITK-SNAP, http://www.itksnap.org (Accessed: 22 February 2013).

[14] A. Enkhbolor, Y.S. Izmantoko, and H.K. Choi, "Comparison of Active Contour and Active Shape Approaches for Corpus Callosum Segmentation," *Journal of Korea Multimedia Society,* Vol. 16, No. 9, pp. 1018-1030, 2013.

Ala'addin Al Shidaifat

received the B.S. degree in Software Engineering from Al-Hussein Bin Talal University, Jordan, in 2011. Currently, he is a master student in Computer Engineering department of Inje University, South Korea, joining Medical Image Technology Laboratory (MITL). His research interests are image enhancement, image segmentation, and image visualization.

Heung-Kook Choi

has gone the undergraduate studying and graduate studying in computer science and engineering at the Department of Electrical Engineering of Linköping University, Sweden (1984-1990) and Ph.D. studying in computerized image analysis at the Center for Image Analysis of Uppsala University, Sweden (1990-1996). He was President of Industry and Academic Cooperation Foundation at Inje University and now he is President of Korea Multimedia Society. His interesting research fields are in computer graphics, virtual reality, and medical image processing and analysis.